

Charge transfer and $2k_F$ vs $4k_F$ instabilities in the NMP-TCNQ molecular metal and $(\text{NMP})_x(\text{Phen})_{1-x}\text{TCNQ}$ solid solutions

Pere Alemany¹, Jean-Paul Pouget², and Enric Canadell³

¹*Departament de Química Física and Institut de Química Teòrica i Computacional (IQTCUB), Universitat de Barcelona, Martí i Franquès 1, 08028 Barcelona, Spain,*

²*Laboratoire de Physique des Solides, Université Paris-Sud, CNRS-UMR 8502, F-91405 Orsay, France,*

³*Institut de Ciència de Materials de Barcelona (CSIC), Campus UAB, 08193 Bellaterra, Spain*

A first-principles DFT study of the electronic structure of the two-chain molecular conductor NMP-TCNQ is reported. It is shown that the charge transfer occurring in this salt is not 1 but $2/3$, finally settling the debate concerning the real charge transfer in this molecular metal. These calculations also lead to a simple rationalization of the three different regimes of $2k_F$ and $4k_F$ CDW instabilities occurring in the solid solutions $(\text{NMP})_x(\text{Phen})_{1-x}\text{TCNQ}$.

PACS numbers: 71.30.+h, 64.70.kt, 71.20.Rv

I. INTRODUCTION

A considerable amount of work has shown that modern density functional theory (DFT) based computational methodologies are reliable enough to cope with many aspects of the electronic structure of molecular conductors. This has paved the way to a deeper understanding at the microscopic level of the always puzzling and challenging physical behavior of many of these low-dimensional materials. For instance, DFT-based approaches have been able to explore the fine details of the electronic structure of 2:1 cation radical molecular conductors such as the Bechgaard and Fabre salts¹⁻³ or several $(\text{BEDT-TTF})_2\text{X}$ salts⁴⁻⁶ where BEDT-TTF stands for bisethylenedithio-tetrathiafulvalene, X is a monovalent anion and the BEDT-TTF layers exhibit different structural arrangements. In all these salts the charge transfer of one hole every two donors is fixed by the stoichiometry. Systems where both donor and acceptor exhibit partially filled bands are considerably more difficult to cope with because the charge transfer depends in these cases on the relative position of both the HOMO (highest occupied molecular orbital) of the donor and the LUMO (lowest unoccupied molecular orbital) of the acceptor, as well as on the widths of the bands generated by these orbitals. Since the charge transfer results from a fine tuning of all these factors, which in turn are strongly linked to the structural details, its determination is thus a delicate problem and yet it has a decisive control on the physical properties of the system. Infrared spectroscopy, optical measurements and x-ray diffuse scattering are the more commonly used experimental techniques to determine the amount of charge transfer, although the final outcome is not always clear-cut. First-principles calculations can thus afford a powerful tool complementing these classical techniques in such cases.

An interesting case is provided by NMP-TCNQ (NMP: N-methylphenazine, TCNQ: 7,7,8,8-tetracyano-p-quinodimethane) which ranks among the earliest synthesized highly conducting 1D organic salts.^{7,8} Its crystal structure is built from segregated donor (NMP) and

acceptor (TCNQ) stacks running along the a direction (Fig. 1a).^{9,10} However, the physical properties of NMP-TCNQ have been the object of considerable controversy. On one hand its electrical conductivity, which exhibits an activated behavior below ~ 225 K, has been interpreted¹¹ as resulting from a progressive localization of the electron wave function because of the intrinsic static disorder due to the asymmetric location of the methyl group of the NMP molecules (see Fig. 1a).¹² On the other hand the magnetic properties have been described as resulting from very strong Coulomb interactions between electrons of the TCNQ stack.^{14,15} These explanations are, however, based on the assumption of a complete^{14,15} or nearly complete^{16,17} charge transfer of one electron from NMP to TCNQ. Assuming a charge transfer of $\rho = 1$, NMP⁺ should be a closed shell molecule and there will be a Mott-Hubbard localization of one electron (spin 1/2) per TCNQ acceptor leading to localized magnetism. With these interpretations in mind, the finding that NMP-TCNQ is subject to two different $2k_F$ charge density wave (CDW) Peierls-like instabilities came as a real surprise.¹³ $2k_F = 1/3a^*$ CDW correlations develop from room temperature to low temperatures, as predicted for the fluctuating Peierls chain¹⁸, then a second $2k_F = 1/6a^*$ CDW develops below 70 K. From the attribution of the $2k_F = 1/3a^*$ CDW to the TCNQ stacks and the $2k_F = 1/6a^*$ CDW to the partially ordered NMP stacks^{12,19} it was deduced that a charge transfer of $\rho = 2/3e$, well below the previous assumptions, should occur in NMP-TCNQ. Vibrational spectroscopy measurements²⁰ for TCNQ were in agreement with this incomplete charge transfer.

NMP-TCNQ forms also particularly interesting $(\text{NMP})_x(\text{Phen})_{1-x}\text{TCNQ}$ solid solutions upon partial substitution of NMP by the neutral closed shell molecule phenazine (Phen). When x decreases the donor band filling vanishes.^{21,22} Thus for $x \sim 0.6$ one moves from a two-band system to a one-band system with a simultaneous crossover from a $2k_F$ CDW to a $4k_F$ CDW instability on the TCNQ stack and a substantial modification of the electronic properties of the solid solution.^{23,24} This

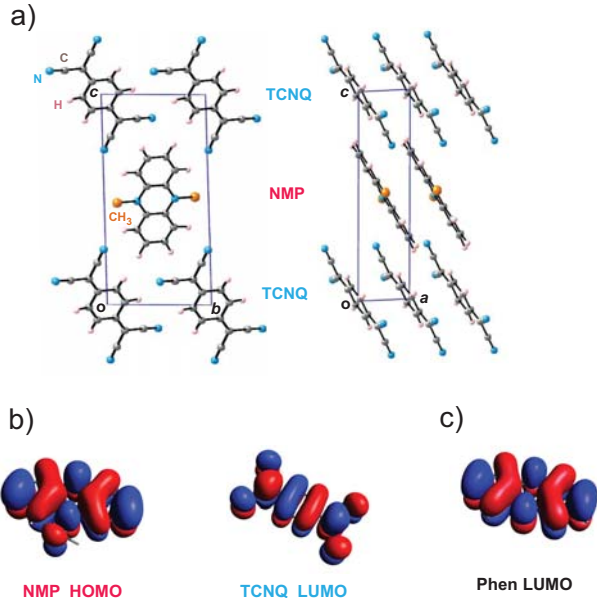


FIG. 1: (a) Crystal structure of NMP-TCNQ. Note that the NMP stacks exhibit positional disorder such that every NMP molecule has only one of the two possible CH_3 groups shown in (a) and the opposite N atom bears a σ lone pair instead. (b) LUMO of TCNQ (center) and HOMO of NMP (left). (c) LUMO of the phenazine molecule.

$2k_F$ to $4k_F$ crossover of the dominant CDW instability suggests that the reduction of screening effects by mobile electrons when the donor band is emptied is a fundamental ingredient to set the long range Coulomb interactions at the origin of the $4k_F$ CDW instability. This finding supports the proposal^{25,26} that the $4k_F$ CDW instability is the fingerprint of a Wigner charge localization in 1D. For $x = 0.5$ one gets a quarter-filled band salt similar to $\text{Qn}(\text{TCNQ})_2$ or $\text{MEM}(\text{TCNQ})_2$ (Qn: quinolinium; MEM: N-methyl-N-Ethyl-morpholinium) which in the presence of dominant electron-electron interactions are subject to a $4k_F$ charge localization and then to a spin-Peierls instability.

In this communication we try to clarify these conflicting scenarios by means of a first-principles DFT study of NMP-TCNQ which clearly confirms that the charge transfer occurring in this salt is not 1 but $2/3$. Our study also provides a simple rationalization of its physical behavior and that of the $(\text{NMP})_x(\text{Phen})_{1-x}\text{TCNQ}$ solid solutions.

II. COMPUTATIONAL DETAILS

Electronic structure calculations were carried out using a numerical atomic orbitals DFT approach^{27,28} as implemented in the SIESTA code.^{29–31} We have used the generalized gradient approximation (GGA) and, in particular, the functional of Perdew, Burke and Ernzerhof.³² Only the valence electrons are considered in

the calculation, with the core being replaced by norm-conserving scalar relativistic pseudopotentials³³ factorized in the Kleinman-Bylander form.³⁴ We have used a split-valence double- ζ basis set including polarization orbitals generated with an energy shift of 10 meV for all atoms.³⁵ The energy cutoff of the real space integration mesh was 250 Ry. The Brillouin zone was sampled using a grid of $(55 \times 3 \times 3)$ k -points³⁶ in the irreducible part of the Brillouin zone for determination of density matrix. The results have been checked to be well converged with respect to the Brillouin zone sampling, real space grid and range of the atomic orbitals. The experimental x-ray crystal structure⁹ disregarding the positional disorder of the methyl groups of NMP was used in the calculations. Test calculations showed that this assumption does not influence the computational results.

III. RESULTS AND DISCUSSION

A. Electronic structure of NMP-TCNQ

The electronic structure of NMP-TCNQ in the vicinity of the Fermi level is built from the LUMO of TCNQ and the HOMO of NMP (Fig. 1b). These two orbitals lead to two bands that cross the Fermi level. As shown in Fig. 2 these bands exhibit a significant dispersion only along the stacks direction. The quasi-1D nature of the band dispersion is clearly proven by the energy dependence of the total and partial density of states (DOS) which exhibit a pronounced divergence at band edges (see Fig. 3). The donor and acceptor bands have parallel dispersions, differing in this sense from the well known TTF-TCNQ case, where the donor and acceptor bands have dispersions of opposite sign.^{37,38} The calculated width of the TCNQ LUMO band is ~ 0.71 eV whereas that of NMP HOMO is of ~ 0.52 eV. The TCNQ bandwidth is comparable to that obtained in the first-principles calculation of the band structure of TTF-TCNQ.^{37,38} Near the Γ point the NMP band has a higher energy than the TCNQ one, while the opposite situation occurs in the vicinity of the X point. Thus the NMP and TCNQ bands tend to cross at some point along the $\Gamma - X$ line. There is in fact an avoided crossing at ~ 0.35 eV above the Fermi level. In this respect NMP-TCNQ differs also from TTF-TCNQ where the band crossing occurs at the Fermi level.^{37,38} It is worth noting that, if we take into account this avoided crossing, the midpoint of the two bands in Fig. 2 practically coincide. This is not usually the case in these charge transfer molecular conductors where the midpoint of the acceptor LUMO usually lies higher in energy than the midpoint of the donor HOMO. In order to understand this feature one must realize that if the methyl group of NMP is removed the phenazine molecule is generated. By doing this, the electron in the NMP HOMO is formally transferred to complete the σ lone pair of the affected N atom and a closed shell molecule is generated. Since the removal of the methyl substituent has only a weak

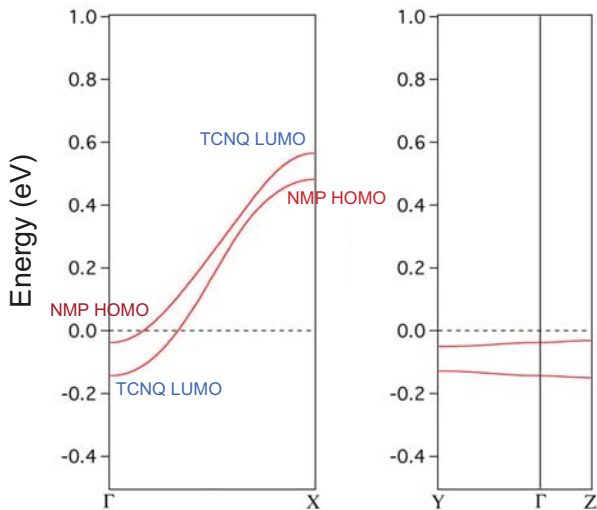


FIG. 2: Band structure for NMP-TCNQ. $\Gamma - X$ is along the stack direction, $\Gamma - Y$ is between neighboring stacks of the same molecules while $\Gamma - Z$ is between neighboring NMP and TCNQ stacks. The zero energy corresponds to the Fermi energy.

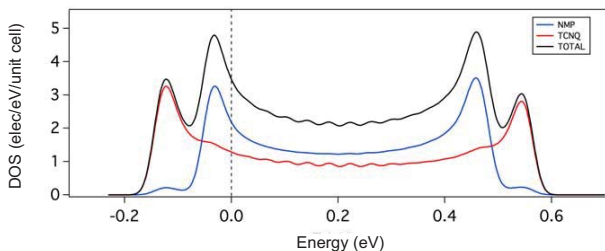


FIG. 3: Calculated density of states (DOS) for NMP-TCNQ and local DOS for the NMP HOMO and TCNQ LUMO in the vicinity of its Fermi energy. The zero energy corresponds to the Fermi energy.

effect on the π system of the molecule, the HOMO of NMP is almost the same orbital as the LUMO of Phen (compare Figs. 1b and 1c). In other words, the HOMO of the donor is very similar to an antibonding molecular orbital of the parent phenazine, so that it must be higher in energy than the HOMO of usual donors.

In NMP-TCNQ there is one electron per formula unit to share between the NMP and the TCNQ bands. With this filling the location of the Fermi level in the band structure of Fig. 2 (left) leads, respectively, to the TCNQ and NMP Fermi wave vectors $k_F^{TCNQ} = 1/6a^*$ and $k_F^{NMP} = 1/12a^*$. Thus the separate nesting of the TCNQ and NMP bands occurs for the $2k_F^{TCNQ} = 1/3a^*$ and $2k_F^{NMP} = 1/6a^*$ wave vectors which exactly correspond to those of the two experimentally observed CDW instabilities of NMP-TCNQ.¹³ Integration of the partial densities of states for the NMP and TCNQ stacks (Fig. 3) also leads to 2/3 electrons on TCNQ and 1/3 electrons on NMP.

Finally, the double sheet Fermi surface of NMP-TCNQ is reported in Fig. 4. The two sheets of this Fermi surface are very weakly warped. Since the avoided crossing lies high enough from the Fermi level every, each sheet can be associated either to the NMP or TCNQ stacks.

Figs. 2 (right) and 4 show that due to the different nodal symmetry of the LUMO and HOMO (see Fig. 1b), the transverse dispersions of the TCNQ and NMP bands have opposite signs. The DFT calculation yields transverse bandwidths of ~ 14 meV and ~ 5 meV along the $\Gamma - Y$ and $\Gamma - Z$ directions, respectively. This leads to an average t_{\perp} of ~ 2.5 meV which is close to the ~ 1.5 meV value estimated from an NMR study of the spin dynamics on the NMP stack.¹⁷ Indeed the same NMR study shows that the spin dynamics in the TCNQ stack has a 1D diffusive behavior at room temperature. The small values of the transverse bandwidth show that the warping of the Fermi surface and associated nesting effects are only thermally relevant below $T < t_{\perp}/\pi \approx 10$ K. Thus the local transverse coupling between $2k_F$ CDWs which develops below 200 K in NMP-TCNQ¹³ must be caused by Coulomb interactions between CDWs as it is generally the case in charge transfer salts.

B. Charge transfer

The present calculations show that contrary to earlier expectations NMP-TCNQ is a partly filled two-band system with a partial charge transfer of 2/3 electrons from NMP to TCNQ due to the fact that the HOMO and LUMO energies of the two species are very close in energy. Very recently a NEXAFS study of the related salts TMP-TCNQ and HMP-TCNQ (TMP/HMP is tetra-/hexa-methoxyppyrene) has provided evidence for a partial charge transfer of 0.13 (0.17) electrons from the TMP (HMP) to the TCNQ.³⁹ It is interesting to remark that the charge of 2/3 electrons per TCNQ molecule is also found in the ternary organic conductor $TMA^+TCNQ^{-2/3}(I_3^-)_{1/3}$.⁴⁰ However whereas NMP-TCNQ is subject to $2k_F$ CDW fluctuations down to low temperature, the single stack TCNQ ternary salt exhibits a sharp metal-to-insulator transition at 150 K accompanied by a tripling of the stack periodicity⁴⁰ with electronic properties bearing some resemblance with those of the charge ordered phase of the Fabre salts.^{41,42}

The present first-principles calculation for NMP-TCNQ leads to a charge transfer coinciding with the experimental results. This may suggest that the noted good performance of usual DFT approaches when the band filling is imposed by the stoichiometry is also extensive to two-chain conductors. The success of a recent DFT study in rationalizing the notoriously complex physical behavior of TTF[Ni(dmit)₂]₂ provides additional support.⁴³ To more thoroughly test the quality of our calculations let us consider the experimentally well-characterized TTF-TCNQ. A calculation performed with the same method and computational details,³⁸ leads to a charge transfer

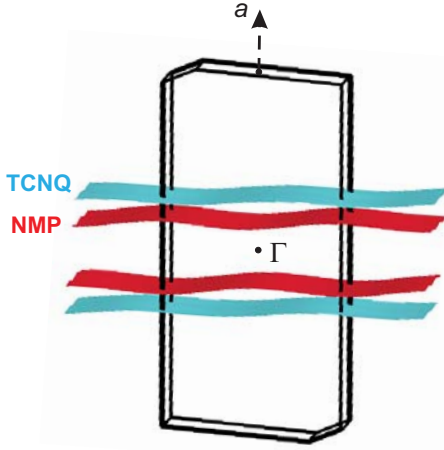


FIG. 4: Calculated Fermi surface for NMP-TCNQ.

in excess by about 30% with respect to the experimental value. Does that overestimation originate from the bands of TTF, TCNQ or both systems? Practically the same result is obtained for LDA and GGA plane-wave based DFT calculations³⁷ so that the failure cannot be attributed to the particular DFT approach used. The width of the TCNQ LUMO band in NMP-TCNQ and TTF-TCNQ is very similar, 0.71 eV and 0.73 eV, respectively. In addition, these values are in good agreement with the experimental estimations for TTF-TCNQ which are around 0.7-0.8 eV.^{44,45} Consequently, the overestimation of charge transfer in TTF-TCNQ is not due to a poor description of the TCNQ LUMO bands within DFT. Our calculated width for the TTF HOMO band in TTF-TCNQ is 0.62 eV, a value similar to those calculated by Sing et al,⁴⁶ 0.625 eV, and Ishibashi et al,³⁷ 0.65 (LDA) or 0.67 (GGA), despite technical differences between the three calculations (Ishibashi et al. use LDA and GGA within a plane-wave pseudopotential method, Sing et al. use LDA within the LAPW approach, and we use GGA with numerical atomic orbitals and pseudopotentials). The calculated width of the TTF HOMO band, 0.62-0.67 eV, does not seem to follow commonly accepted ideas according to which the dispersion of the TTF HOMO bands in TTF-TCNQ should be clearly smaller than that of the TCNQ LUMO bands. In fact, experimental estimations suggest values around 0.4-0.45 eV.^{44,45} This situation contrasts with the good agreement between calculated DFT and experimental estimations of the charge transfer for the TTF[Ni(dmit)₂]₂ and TTF[Pd(dmit)₂]₂ molecular conductors.⁴³ The important difference is that the width of the TTF HOMO bands is noticeably larger in these compounds, 0.89 eV and 1.18 eV, respectively. Both TTF[Ni(dmit)₂]₂ and TTF[Pd(dmit)₂]₂ are room temperature metals. In contrast, the observation of a $4k_F$ CDW instability located on the TTF chains of TTF-TCNQ by X-ray diffuse scattering experiments⁴⁷ suggests that electronic correlations are important in the TTF stacks of this salt. We have

found that in such case the GGA+U approach⁴⁸ with $U = 4$ eV for the $3p$ electrons of S provides a good description of the band widths and charge transfer of TTF-TCNQ and other related two-chain conductors, thus extending the usefulness of DFT for the study of these systems.

C. The $(\text{NMP})_x(\text{Phen})_{1-x}$ TCNQ solid solution

The calculated band structure for NMP-TCNQ can also account for the evolution of the band filling in $(\text{NMP})_x(\text{Phen})_{1-x}$ TCNQ solid solutions if one assumes that varying the amount of neutral Phen molecule results only in a change of the number of electrons (x) that populate the conduction band without affecting its dispersion. As mentioned before, the phenazine molecule is not only structurally very similar to NMP, but possesses a LUMO that is topologically equivalent to the HOMO of NMP (Figs. 1b (left) and 1c). Consequently, the overlap integrals should be very similar when the replacement of Phen for NMP occurs in the chains. Although the site energies are in principle not exactly the same, when Phen and NMP occur in a mixed stack with excellent overlap between the π orbitals of the two molecules, they should not differ noticeably. Thus a rigid band model should capture the essential physics of the system. In such a model it is easy to calculate the evolution of the charge transfer with x . If one denotes $\rho_{\text{TCNQ}} = 4k_F^{\text{TCNQ}}$ and $\rho_{\text{NMP}} = 4k_F^{\text{NMP}}$ (with k expressed in units of a^*) the number of electrons per TCNQ and NMP molecules respectively in the partially filled bands of this system, it follows that

$$\rho_{\text{TCNQ}} + \rho_{\text{NMP}} = x \quad (1)$$

In agreement with the band structure of Fig. 2, if in the energy range of interest one takes a quadratic dispersion for the NMP band and a linear dispersion for the TCNQ band, the Fermi energy with respect to the bottom of the NMP band for the NMP and TCNQ bands is

$$\epsilon_F = \frac{\hbar^2(k_F^{\text{TCNQ}})^2}{2m}, \quad (2)$$

and

$$\epsilon_F = \hbar v_F(k_F^{\text{TCNQ}} - k_c), \quad (3)$$

respectively. In eq. (3) $k_c \sim 0.145 a^*$ is the wave vector for which the TCNQ band reaches the minimum energy of the NMP band. By equating (2) and (3) it is possible to obtain a simple relation between ρ_{TCNQ} and ρ_{NMP} :

$$\rho_{\text{NMP}}^2 = C(\rho_{\text{TCNQ}} - x_c), \quad (4)$$

with $C = \frac{8mv_F}{\hbar} \approx 1.1$ and $x_c = 4k_c \approx 0.58$. Note that for $x \geq x_c$ both bands are partially filled. Using eqs. (1) and (4) one gets:

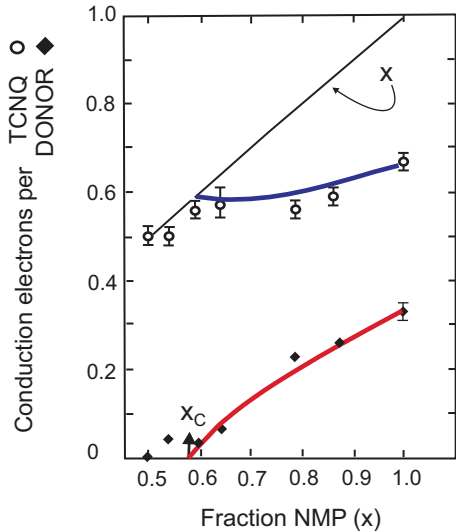


FIG. 5: Number of electrons per TCNQ and donor molecule as a function of x in the $(\text{NMP})_x(\text{Phen})_{1-x}\text{TCNQ}$ solid solutions. The continuous blue and red lines are the charges calculated using the rigid band model discussed in the text. Experimental points taken from references ^{21,22}. The solid black line gives the total conduction electrons per formula unit available.

$$\rho_{\text{NMP}} = C \left[-\frac{1}{2} + \sqrt{\frac{1}{4} + \left(\frac{x - x_c}{C}\right)^2} \right], \quad (5)$$

and

$$\rho_{\text{TCNQ}} = x - \rho_{\text{NMP}}. \quad (6)$$

For $x \leq x_c$ only the TCNQ band is partially filled and thus, $\rho_{\text{TCNQ}} = x$. As shown in Fig. 5, the ρ_{TCNQ} (blue line) and ρ_{NMP} (red line) calculated through the above expressions nicely account for the experimental values determined in the $(\text{NMP})_x(\text{Phen})_{1-x}\text{TCNQ}$ solid solution.^{21,22}

On the basis of the above analysis three different situations can be distinguished:

(i) For $x \sim 1$, the carriers are delocalized for each type of stacks which then exhibit a $2k_F$ CDW instability.

(ii) For $0.5 \leq x \leq x_c \approx 0.58$ all the electrons are in the TCNQ stacks which are surrounded by $\text{NMP}^+/\text{Phen}^0$ mixed stacks.⁴⁹ The Coulomb repulsions of the electrons

located on the TCNQ stack are not well screened because there are no mobile carriers on the $\text{NMP}^+/\text{Phen}^0$ stack and the electron density on the TCNQ is low. Under such conditions the $4k_F$ CDW instability on the TCNQ stacks is dominant and tends to achieve Wigner-type charge localization.

(iii) In between these two types of behavior the salt is subject to two types of disorder: positional disorder of the methyl group in NMP and NMP/Phen substitution disorder. Such disorder suppresses the $2k_F$ CDW instability on the NMP stack.¹⁹ The electron density on the NMP/Phen disordered stack decreases with x and the electrons tend to localize in regions with excess of NMP. In contrast the electrons will remain delocalized on the TCNQ stack which still presents the $2k_F$ CDW instability together with growing $4k_F$ CDW correlations when x approaches x_c .

These three regimes provide a simple rigid band type rationalization of the experimental results noted in the introduction for these solid solutions.

IV. CONCLUDING REMARKS

A first-principles DFT study of the electronic structure of NMP-TCNQ leads to a charge transfer of $2/3$ electrons and thus settles the debate concerning the real charge transfer in this room temperature metal. These calculations lead also to a simple rigid band scheme rationalization of the three different types of CDW instabilities occurring in $(\text{NMP})_x(\text{Phen})_{1-x}\text{TCNQ}$ solid solutions. A comparison of these results with those for TTF based two-chain molecular conductors suggests that LDA+U or GGA+U approaches are needed when the calculated band width of the TTF HOMO band is relatively narrow (0.6-0.7 eV) but otherwise the usual LDA and GGA functionals provide an appropriate description.

Acknowledgments

One of us (JPP) thanks A. J. Epstein for collaborations in the study of the $(\text{NMP})_x(\text{Phen})_{1-x}\text{TCNQ}$ system. This work was supported by MINECO (Spain) through Grants FIS2012-37549-C05-05 and CTQ2011-23862-C02-02, as well as Generalitat de Catalunya (2014SGR301 and XRQTC). E.C. acknowledges support of the Spanish MINECO through the Severo Ochoa Centers of Excellence Program under Grant SEV-2015-0496.

¹ Ishibashi S., Sci. Technol. Adv. Mater. **10**,024311 (2009).
² Jacko A.C., Feldner H., Rose E., Lissner F., Dressel M., Valenti R., and Jeschke H. O., Phys. Rev. B **87**, 155139 (2013).
³ Alemany P., Pouget J.-P., and Canadell E., Phys. Rev. B **89**, 155124 (2014).

⁴ Foury-Leylekian P., Pouget J.-P., Lee Y.-J., Nieminen R. M., Ordejón P., and Canadell E., Phys. Rev. B **82**, 134116 (2010).

⁵ Alemany P., Pouget J.-P., and Canadell E., J. Phys.:Condens. Matter **27**, 465702 (2015).

⁶ Alemany P., Pouget J.-P., and Canadell E., Phys. Rev. B

- 85**, 195118 (2012).
- ⁷ Melby L.R., *Canad. J. Chem.* **43**, 1448 (1965).
- ⁸ Schegolev I. F., *Phys. Stat. Sol. (b)* **12**, 4 (1972).
- ⁹ Fritchie C. J., *Acta Crystallogr.* **20**, 892 (1966).
- ¹⁰ Morosin B., *Phys. Lett.* **53A**, 455 (1975).
- ¹¹ Bloch A. M., Weisman R. B., and Varma C. M., *Phys. Rev. Lett.* **28**, 753 (1972).
- ¹² This assertion does not rely on exact structural information because NMP orders in the (a,b) plane uniformly along b and in alternate manner along a (see ref.¹³). The alternate order is disrupted by stacking faults in the a direction. From the data of ref.¹³ the typical size of a staggered ordered domain is estimated to be 40 Å along a , which corresponds to about two $(2k_F^{NMP})^{-1}$ CDW wave-lengths. NMP donors are disordered in the c direction.
- ¹³ Pouget J. P., Metgert S., Comès R., and Epstein A. J., *Phys. Rev. B* **21**, 486 (1980).
- ¹⁴ Epstein A. J., Etemad S., Garito A. F., and Heeger A. J., *Solid State Commun.* **9**, 1803 (1971).
- ¹⁵ Epstein A. J., Etemad S., Garito A. F., and Heeger A. J., *Phys. Rev. B*, **5**, 952 (1972).
- ¹⁶ Butler M. A., Wudl F., and Soos Z. G., *Phys. Rev. B* **12**, 4708 (1975).
- ¹⁷ Devreux F., Guglielmi M., and Nechtschein M., *J. Phys. (Paris)***39**, 541 (1978).
- ¹⁸ Pouget J. P., *Z. Kristallogr.* **219**, 711 (2004).
- ¹⁹ The assignment of the $2k_F = 1/6a^*$ CDW instability to the NMP stack can be done unambiguously from the vanishing of this instability with the NMP/Phen substitution disorder in the $(\text{NMP})_x(\text{Phen})_{1-x}$ TCNQ solid solution.
- ²⁰ Kuzmany H., and Elbert M., *Solid State Commun.* **35**, 597 (1980).
- ²¹ Epstein A. J., Miller J. S., Pouget J. P., and Comès R., *Phys. Rev. Lett.* **47**, 741 (1981).
- ²² Pouget J. P., Comès R., Epstein A. J., and Miller J. S., *Mol. Cryst. Liq. Cryst.* **85**, 203 (1982).
- ²³ Epstein A. J. and Miller J. S. in *The Physics and Chemistry of Low dimensional Solids* Alcacer. L., Ed., Reidel, Boston (1980) p. 339.
- ²⁴ Epstein A. J., Kaufer J. W., Rommelmann H., Howard I. A., Conwell E. M., Miller J. S., Pouget J. P., and Comès R., *Phys. Rev. Lett.* **49**, 1037 (1982).
- ²⁵ Kondo J. and Yamaji K., *J. Phys. Soc. Jpn.***43**, 424 (1977).
- ²⁶ Hubbard J., *Phys. Rev. B* **17**494 (1979).
- ²⁷ Hohenberg P. and Kohn W., *Phys. Rev.* **B136**, 864 (1964).
- ²⁸ Kohn W. and Sham L. J., *Phys. Rev.***A140**, 1133 (1965).
- ²⁹ Soler J. M., Artacho E., Gale J. D., García A., Junquera J., Ordejón P., and Sánchez-Portal D., *J. Phys.: Condens. Matter* **14**2002, 2745 (2002).
- ³⁰ Artacho E., Anglada E., Diéguez O., Gale J. D., García A., Junquera J., Martín R. M., Ordejón P., Pruneda J. M., Sánchez-Portal D., and Soler J. M., *J. Phys.: Condens. Matter* **20**, 064208 (2008).
- ³¹ For more information on the SIESTA code visit: <http://icmab.cat/leem/siesta/>
- ³² Perdew J. P., Burke K. , and Ernzerhof M., *Phys. Rev. Lett.* **77**, 3865 (1966).
- ³³ Troullier N. and Martins J. L., *Phys. Rev. B*, **43**, 1993 (1991).
- ³⁴ Kleinman L. and Bylander D. M., *Phys. Rev. Lett.* **48**, 1425 (1982).
- ³⁵ Artacho E., Sánchez-Portal D., Ordejón P., García A., and Soler J. M., *Phys. Stat. Sol. (b)* **215**, 809 (1999).
- ³⁶ Monkhorst H. J. and Pack J. D., *Phys. Rev. B* **13**, 5188 (1976).
- ³⁷ Ishibashi S. and Kohyama M., *Phys. Rev. B* **62**, 7839 (2000).
- ³⁸ Fraxedas J., Lee Y.-J., Jiménez I., Gago R., Nieminen R. M., Ordejón P., and Canadell E., *Phys. Rev. B* **68**, 195115 (2003).
- ³⁹ Medjanik K., Chercka D., Nagel P., Merz M., Schuppler S., Baumgarten M., Müllen K., Nepijko S. A., Elmers H.-J., Schönhense G., Jeschke H. O., and Valenti R., *J. Am. Chem. Soc.* **134**, 4694 (2002).
- ⁴⁰ Gallois B., Gaultier J., Pouget J. P., Coulon C., and Filhol A., *J. Phys. (Paris)* **44**, C3-1307 (1983).
- ⁴¹ Coulon C. and Clérac R., *Chem. Rev.* **104**, 5655 (2004).
- ⁴² When $\rho = 2/3$, the $2k_F$ and $4k_F$ critical wave vectors are equivalent within one reciprocal wave vector ($4k_F = a^* - 2k_F$). For this special band filling it is thus difficult to discriminate between the CDW properties due to a $2k_F$ Peierls or to a $4k_F$ charge localized Wigner ground state. The study of the $(\text{NMP})_x(\text{Phen})_{1-x}$ TCNQ solid solutions shows by continuity that the TCNQ stack of NMP-TCNQ is primarily subject to a $2k_F$ CDW-Peierls instability. The reduction of the inter-chain screening of Coulomb repulsions in the single stack TMA-TCNQ-I salt could favor $4k_F$ charge localization on the TCNQ stack as suggested by ESR measurements⁴¹. Note that with $4k_F$ equivalent to $2k_F$, the Wigner-like charge localized transition does not lead to a spin-charge decoupling. Thus for the $2/3$ band filling, and contrary to what is observed in quarter-filled band systems, the charge localization should be accompanied by a spin gap opening.
- ⁴³ Kaddour W., Monteverde, M., Auban-Senzier P., Raffy H., Pouget J.-P., Pasquier C. R., Alemany P., Canadell E., and Valade L., *Phys. Rev. B* **90**, 205132 (2014).
- ⁴⁴ Jérôme D. and Schulz H., *Adv. Phys.* **31** 299 (1982).
- ⁴⁵ Jacobsen C. S., *Mat. Fys. Medd. K. Dan. Vidensk. Selsk.* **41**, 251 (1985).
- ⁴⁶ Sing M., Claessen R., Finteis Th., Hao S., Hüfner S., and Blaha P., *J. Electron Spectrosc. Relat. Phenom.* **114-116**, 717 (2001).
- ⁴⁷ Pouget J. P. in *Semiconductors and Semimetals* Conwell, E. Ed., vol**27**, Academic Press, New York (1988) p. 88.
- ⁴⁸ Dudarev S. L., Botton G. A., Savrasov S. Y., Humphreys C. J., and Sutton A. P., *Phys. Rev. B* **57**, 1505 (1988).
- ⁴⁹ For $x = 0.5$ NMP and Phen exhibit a staggered order (see ref.²²).